SOLAR ENERGY

Bacterial Foraging Algorithm based solar PV parameter estimation

N. Rajasekar *, Neeraja Krishna Kumar, Rini Venugopalan

School of Electrical Engineering, VIT University, Vellore, India

Abstract

The abundance and non-polluting nature of solar energy has aroused the interest of many researchers. This worldwide attention of photovoltaic panels has led to the need of generating accurate model for solar photovoltaic (PV) module before proceeding to the installation part. However, accurate modeling of solar PV characteristics is difficult; since the manufacturer's datasheet provides only four values such as V_{mp}, I_{mp}, V_{oc}, and I_{sc}. Further, for accurate modeling precise estimation of model parameters at different environmental conditions are very essential. On the other hand, optimization technique is a very powerful tool to obtain solutions to complex non-linear problems. Hence, in this paper, Bacterial Foraging Algorithm is proposed to model the solar PV characteristics accurately. A new equation has been evolved to determine the values of V_{oc}, V_{mp} accurately; since these values decides the closeness of the simulated characteristics. Model parameters are extracted for three different types of solar PV panels. A systematic evaluation and performance comparison of Bacterial Foraging Algorithm with other optimization techniques such as Genetic Algorithm and Artificial Immune System has been done and the best computational technique is derived based on performance criteria such as accuracy, consistency, speed of convergence and absolute error. Extensive computations are carried out for the proposed method, as well as for Genetic Algorithm and Artificial Immune System to substantiate the findings.
© 2013 Elsevier Ltd. All rights reserved.

Keywords: Bacterial Foraging Algorithm; Genetic Algorithm; Artificial Immune System; Solar PV modeling

1. Introduction

The renewable energy sources available to us are abundant and very suitable to meet the ever increasing requirement of energy by mankind without causing any harmful effects to the nature. Moreover, the fossil fuels used across the world are a major cause of global warming and air pollution. Among the various available renewable energy resources, solar energy has attained worldwide recognition; because of its inexhaustibility, pollution-free nature, zero maintenance, zero noise and reliability. However, solar power is not popular because of its high installation cost and poor panel efficiency. Further, in contrast, continuous reduction in solar panel costs has attracted the attention of researcher's towards solar power generation. Modeling solar Photo Voltaic (solar PV) characteristics using simulation software's like MATLAB, PSPICE is a major concern to the researchers; since the behavior of the PV fed system largely relies on the accuracy of the predicted solar PV characteristics.

The accuracy of the solar PV characteristics mainly depends on the model parameter values. A reliable and efficient simulation model of solar PV is vital before proceeding to the installation part. Generally, there are two approaches to realize the characteristics of solar PV; Single diode model (Villalva et al., 2009; De Soto et al., 2006; Walker, 2001; Ishaque and Salam, 2011; Macabebe et al., 2011) and Double diode model (Ishaque et al., 2011a; Ishaque et al., 2011b). The single diode model is popular

---

* Corresponding author. Tel.: +91 9952362301.
  E-mail addresses: natarajanrajasekar@gmail.com (N. Rajasekar), neerajakk@rediffmail.com (N. Krishna Kumar), rini.venugopalan@yahoo.co.in (R. Venugopalan).

because of its easy modeling and reduced number of model parameters. For modeling the solar panel using single diode model, various model parameters such as photo-generated current (I_{pv}), diode saturation current (I_o), diode ideality factor (a), series resistance (R_s) and shunt resistance (R_p) are to be determined. The determination of the exact values of these model parameters is very crucial; since it decides the accuracy of the predicted solar panel characteristics. However, the nonlinearity involved in the solar PV characteristics imposes difficulty towards the extraction of model parameters. Generally, analytical and numerical methods have been used to obtain the model parameters (Chan and Phang, 1987; Romero et al., 2012; Ortiz-Conde et al., 2006; Jian and Kapoor, 2004). However, determination of parameters using the above methods is tedious, complex and time consuming.

On the other hand, bio-inspired algorithms are excellent choice to deal with nonlinear, non-differentiable and stochastic problems without involving excessive mathematical computations. Efforts have been made in the recent past applying various optimization algorithms such as Genetic Algorithm (GA), Particle Swarm Optimization (PSO), and Harmony Search algorithm (HS) to predict the solar PV characteristics accurately (Jian and Kapoor, 2004; Jervase et al., 2001; Moldovan et al., 2009; Zagrouba et al., 2010; Costa et al., 2010; Askarzadeh and Rezazadeh, 2012; Ye et al., 2009; Macabebe et al., 2011). However, in literature, Bacterial Foraging (BFA) and Artificial Immune System (AIS) have not been implemented for the parameter extraction and there have not been many studies taken place for the detailed analysis of the performance comparison using different optimization approaches. Hence, in this paper, BFA is proposed to predict the solar PV characteristics accurately. Further, the three optimization methods namely BFA, GA, AIS are evaluated for three different types of PV modules which are mono-crystalline, thin film and multi-crystalline. In addition, the BFA results are compared with GA and AIS method.

The remaining section of the paper is organized as follows: Section 2 explains the modeling of solar PV modules. Section 3 describes the formulation of objective function. In addition, explanation about newly derived equations for determination of V_{oc}, I_{sc} is presented. Section 4 explains the steps involved in application of three optimization techniques (GA, AIS and BFA) for solving the above framed optimization problem. Results obtained are discussed in Section 5.

2. Modeling of PV module

Many models have been developed so far to depict the solar characteristics accurately (Jian and Kapoor, 2004). Among these, the most important and widely used models are: Double diode model and Single diode model. Even though double diode model is the most accurate one, the high complexity hinders its common usage. Therefore, Single diode model is used in this paper.

2.1. Single diode model

Single-diode model is the most commonly used electric model for representing the behavior of a solar PV module due its average complexity and accurate results. The ideal model comprises of a current source I_{pv} connected in parallel with a diode. But, practically there is an effect of resistance in series along the current path through the semiconductor material, metal grid, contacts which are added together and denoted as series resistor R_s. Apart from this, there is a loss due to the leakage of current through a resistive path in parallel with device which is represented by a parallel resistor R_p. The practical single diode model is depicted in Fig. 1.

Applying KCL the module output current can be written as:

$$I = I_{pv} - I_D - \frac{V_D}{R_p} \quad (1)$$

where I_D is the diode current and V_D is the diode voltage.

The basic diode current equation can be written as:

$$I_D = I_o(e^{V_D/\alpha V_t} - 1) \quad (2)$$

where a is the diode ideality factor and V_t is the thermal voltage which is given by the equation:

$$V_t = N_s kT/q \quad (3)$$

where k is the Boltzmann constant, T is the cell temperature in Kelvin, q is the electron charge, N_s is the number of cells in series. Using KVL, the output voltage of the module can be written as:

$$V = V_D - IR_s \quad (4)$$

Therefore, from the above discussion, in single-diode model, I_{pv}, I_o, R_s, R_p, and a are the five model parameters that need to be computed.

3. Problem formulation

As described earlier, to model solar PV characteristics using single diode model, it requires the computation of five model parameters namely I_{pv}, I_o, R_s, R_p, and a. In this paper, to reduce computational complexity, the values of I_{pv} and I_o are calculated analytically; whereas the remaining values such as R_s, R_p, and a are computed using optimization techniques. These values are adjusted in such a way that the error between the computed characteristics
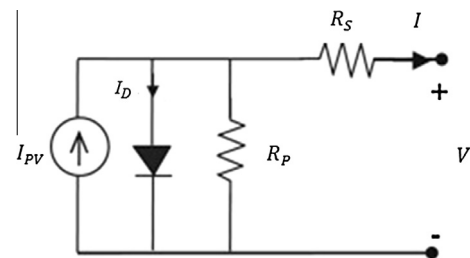

Fig. 1. Single diode model for PV modeling.

and the actual characteristics is minimized. The parameter values vary according to the change in environmental conditions particularly temperature and irradiation. It is worth mentioning that, in this paper, the model parameter values are found making use of only the available manufacture's datasheet information.

The photo current of a particular solar PV panel is determined using:

$$I_{pv} = (I_{scn} + k_i dT)\frac{G}{G_n} \qquad (5)$$

where I_{scn} is the short circuit current at STC, k_i is the current temperature coefficient and its value is available in the respective panel datasheet. G_n is the irradiation at STC i.e. 1000 W/m^2 and G is the particular irradiation to which the panel is exposed. In (5), $dT = T - T_n$, where T_n is the temperature at STC condition i.e. 25 °C and T is the surface temperature of the panel. The reverse saturation current is obtained using equation given in Ishaque and Salam (2011) and is given below:

$$I_o = \frac{I_{pv}}{\exp[(V_{oc} + k_v dT)/a/V_t] - 1} \qquad (6)$$

In (Ishaque and Salam, 2011), Eqs. (7) and (8) were utilized to determine the values of open circuit voltage (V_{oc}) and voltage at maximum power (V_{mp})

$$V_{oc} = V_{ocn} + V_t \ln\left(\frac{G}{G_n}\right) + k_v dT \qquad (7)$$

$$V_{mp} = V_{mpn} + V_t \ln\left(\frac{G}{G_n}\right) + k_v dT \qquad (8)$$

These values are unique to each panel and it determines the accuracy of the result. So these values are needed to be accurately determined. However, when tested, the above equations failed to produce the accurate results. Hence, the above two equations are need to be modified to take care of irradiation change as well as temperature variation. This can be done by adding an extra term to Eqs. (7) and (8) as given below:

$$V_{oc} = V_{ocn} + V_t \ln\left(\frac{G}{G_n}\right) + k_v dT + \alpha \log\left(\frac{G}{G_n}\right) \qquad (9)$$

$$V_{mp} = V_{mpn} + V_t \ln\left(\frac{G}{G_n}\right) + k_v dT + \beta V_t \log\left(\frac{G}{G_n}\right) \qquad (10)$$

In the above equations, α and β are two coefficients of the panel which must vary with temperature and irradiation so that the exact PV curve can be obtained.

The current at maximum power point Imp is given by:

$$I_{mp} = I_{mpn} \ln\left(\frac{G}{G_n}\right)\{1 + k_i dT\} \qquad (11)$$

The computed value of V_{oc} and V_{mp} using the above developed equations matches accurately with the manufacturer's datasheet and it will vary according to the type of solar panel. The α, β values are taken as 0.9 and 1.65 respectively to match values of V_{oc} and V_{mp} with Shell

solar characteristics. However, the above equations can be modified for any panel simply by changing the last term of Eqs. (9) and (10).

From Fig. 2 at Maximum Power Point (MPP), the derivative of the power with respect to voltage is equal to zero. i.e. $\frac{dP}{dV} = 0$.

The power equation is written as $P = VI$. Applying condition for MPP the above equation changes to

$$\frac{dP}{dV} = V\frac{dI}{dV} + I \qquad (12)$$

The term $\frac{dP}{dV}$ should be made as zero in order to get maximum power. So, the RHS of Eq. (12) is equated to zero.

$$V\frac{dI}{dV} + I = 0 \qquad (13)$$

$$\text{i.e.}, \frac{dI}{dV} + \frac{I}{V} = 0 \qquad (14)$$

The objective function, the function to be minimized, is obtained from Eq. (14); which is similar to (Ishaque and Salam, 2011) and it is given below:

$$J = \left|\frac{dI}{dV}\right|_{(V_{mp}, I_{mp})} + \frac{I_{mp}}{V_{mp}} \qquad (15)$$

In the above equation, $\left|\frac{dI}{dV}\right|_{(V_{mp}, I_{mp})}$ term can be obtained by taking the derivative of the basic current equation of the single diode model given in Eq. (1), which is given by:

$$\left|\frac{dI}{dV}\right|_{(V_{mp}, I_{mp})} = \frac{I_o \Gamma \exp\{\Gamma(V_{mp} + I_{mp}R_s)\} - G_p}{1 + I_o \Gamma R_s \exp\{\Gamma(V_{mp} + I_{mp}R_s)\} - G_p R_s} \qquad (16)$$

where $G_p = 1/R_p$ and $\Gamma = 1/aV_t$

The best solution is obtained with regard to a particular value called fitness value which is evaluated after each iteration.

4. Analysis of various optimization techniques

Overview of various optimization techniques applied in this work is presented in this section and it includes Genetic Algorithm, Artificial Immune System and Bacterial Foraging Algorithm. All the methods share the property of bio-inspired algorithms, population based method and
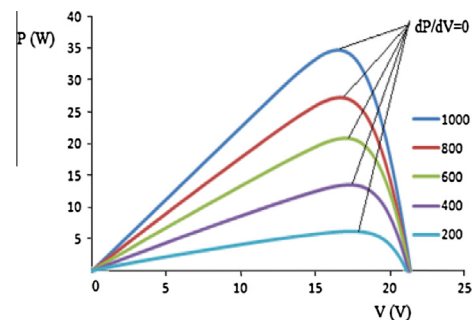

Fig. 2. *P–V* characteristics.

having the common characteristics of starting with a random initial guess of R_s, R_p, and a finally converging to an optimal value. It is noteworthy to mention that, BFA and AIS have not been implemented in the past for the parameter extraction.

4.1. Genetic Algorithm

The Genetic Algorithm was initially proposed by Holland (Holland, 1975). After that many authors (Goldberg, 2000; Michalewicz, 1994) have modified the existing one and improved genetic algorithms are proposed. The genetic algorithm for the parameters extraction of solar panels has already been implemented in the work presented in Jervase et al. (2001), Moldovan et al. (2009), Zagrouba et al. (2010). The Darwin's theory 'The survival of fittest' is the basic mechanism of GA which automatically selects healthiest population among a set of population. Pseudo code explaining various steps of genetic algorithm is explained below:

Step 1: Generate an initial random population;
Step 2: Evaluate fitness of each individual's in the population;
Step 3: Select parents from the population,
    Running crossover operators: Recombine (mate) parents to produce children;
    Running Mutation operators: Randomly alter one or more genes of a child;
Step 4: Evaluate fitness of the children;
Step 5: Replace some or all of the population by the children;
Step 6: Loop until a satisfactory solution has been found,
    Go to step 3;
Step 7: Terminate the search if the best solution is found.

The following GA parameters are used in this work:

Population size = 100
Maximum generations = 250
Crossover rate = 0.8
Mutation rate = 0.3

The flowchart explaining the GA processes is shown in Fig. 3.

4.2. Artificial Immune System

Artificial Immune System (AIS) has attained worldwide attention because of its ability to solve complex optimization problems (Farmer et al., 1986; Xiaoping et al., 2003; Fugang, 2010). AIS imitates immune system of human body by fighting bacteria, viruses and other foreign particles. The antigen antibody reaction is the basic mechanism behind AIS which yields better performance in the field of optimization. The immune cells present in the human body are called
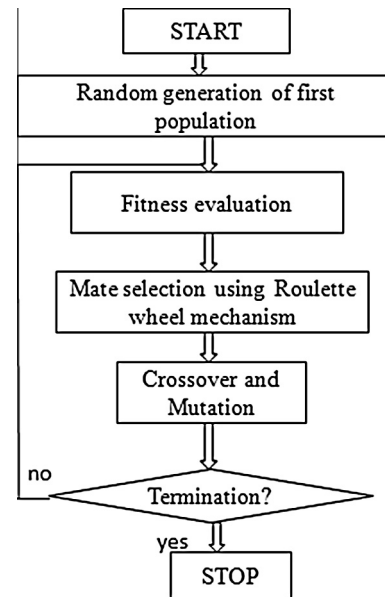

Fig. 3. Flowchart of GA.

as antibodies which fight against the antigen, the foreign particles in the human body. Various steps involved in AIS can be explained with the help of following pseudo code:

- Step 1. Identification of antigen: The objective function to be minimized and the constraints associated with that is considered as the antigen.
- Step 2. Creation of initial antibody population: The initial population of antibody is generated randomly.
- Step 3. Analysis of objective function: Each antibody is allowed to interact with the antigen and the fitness value is evaluated.
- Step 4. Affinity calculation: The affinity between the antibody and antigen is determined. The antibody with higher affinity towards antigen, i.e. the 'healthy' antibody which has the ability to annihilate the antigen are added to the memory cells.
- Step 5. Calculation of selection probability: The selection probability is evaluated based on fitness probability and density probability and is given by:

Fitness probability can be written as:

$$p_f = f(x_i) \Big/ \sum_{j=1}^{S} f(x_j) \qquad (17)$$

The density of antibody is the proportion of antibodies with same affinity to the total antibodies is

$p_d = 1/s(1 - t/s)$ for antibodies with highest density
$p_d = 1/s(1 + (t^2/s^2 - st))$ for other $s - t$ antibodies

where s is the total number of antibodies.
The selection probability is the sum of fitness probability and density probability which is given by:

$$p = \alpha p_f + (1 - \alpha)p_d \qquad (18)$$

where $0 < \alpha < 1$

The antibodies with higher selection probability are selected for the next generation. The highest selection probability is obtained for those antibodies with high fitness probability and low density probability.

- *Step* 6. Crossover and mutation: The crossover and mutation process in AIS is similar to GA. Go to step 3 till the termination criteria is reached.

The following AIS parameters are used in this work:

Population size $= 100$
Maximum generations $= 250$
Crossover rate $= 0.8$
Mutation rate $= 0.3$
$\alpha = 0.4$

The graphical form of the above procedural steps is presented in the flowchart Fig. 4.

4.3. Bacteria Foraging Algorithm

Bacteria Foraging Algorithm (BFA) was proposed by Passino and a new addition to the family of nature-inspired optimization algorithms (Passino, 2002). By the laws of

natural selection, animals which were having poor foraging technique will be eliminated or will be converted to good ones after many generations (Passino, 2002). Many researchers have made use of this technique as an optimization tool (Mishra, 2005; Mishra and Bhende, 2007; Eslamian, 2009). Escherichia coli bacteria present in human intestine also undergo foraging strategy and can be explained by four processes, namely chemotaxis, swarming, reproduction, elimination and dispersion. The following section describes how the BFA is designed and applied to the present problem.

Step 1: Initialization
  (1) S – Number of bacteria
  (2) P – Number of parameters to be optimized i.e., values of model parameter such as R_s, R_p, and a;
  (3) N_s – Swimming length, the maximum number of steps each bacteria swims before tumbling
  (4) N_c – Number of iterations to be undertaken in a chemotactic loop;
  (5) N_{re} – Maximum number of reproduction to be undertaken;
  (6) N_{re} – Maximum number of elimination and dispersal;
  (7) P_{ed} – Probability of elimination and dispersal;
  (8) $C(i)$ – Unit run length for bacterium and is assumed as constant in our case;
  (9) Values of $d_{attract}$, $w_{attract}$, $h_{repelent}$, $w_{repelent}$
  (10) θ^i, $i = 1, 2, 3, \ldots\ldots, S$ – Random Swim direction
Step 2: Elimination–dispersal loop $l = l + 1$
Step 3: Reproduction loop $k = k + 1$
Step 4: Chemotaxis loop $j = j + 1$
  (A) For each bacterium $i = 1, 2, 3, \ldots\ldots, S$, compute objective function $J(i, j, k, l)$.
    a. Let $J_{sw}(i, j, k, l) = J(i, j, k, l) + J_{cc}(\theta^i(j, k, l), P(j, k, l))$
    where

$$J_{CC} = \sum_{i=1}^{S}\left[-d_{attract}\exp\left(-w_{attract}\sum_{m=1}^{P}(\theta_m - \theta_m^i)^2\right)\right]$$
$$+\sum_{i=1}^{S}\left[-h_{repelent}\exp\left(-w_{repelent}\sum_{m=1}^{P}(\theta_m - \theta_m^i)^2\right)\right]$$

    b. Let $J_{last} = J_{sw}(i, j, k, l)$, to save this value since we find a better cost via a run.
    c. End of the loop
  (B) Tumble: Generate a random vector $\Delta(i), \in \Re^p$ with each element being a random number in the range of $[-1, 1]$
  (C) Move:

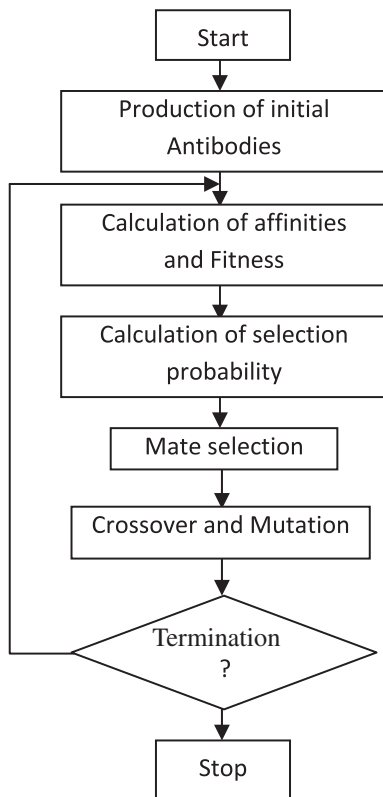$$\text{Let } \phi(i) = \frac{\Delta(i)}{\sqrt{\Delta^T(i)\Delta(i)}}$$

Fig. 4. Flowchart of AIS.

$$\theta^i(j+1, k, l) = \theta^i(j, k, l) + C(i)\phi(i)$$

This results in a step size $C(i)$ in the direction of the tumble for the i th bacterium.

(D) Compute $J(i, j+1, k, l)$ and then let $J_{sw}(i, j+1, k, l) = J(i, j+1, k, l) + J_{cc}(\theta^i(j+1, k, l), P(j+1, k, l))$

(E) Swim:
    a. Let $m = 0$ (counter length for swim)
    b. While $m < N_S$
        i. Let $m = m + 1$
        ii. If $J_{sw}(i, j+1, k, l) < J_{last}$
        then $J_{last} = J_{sw}(i, j+1, k, l)$
        $\theta^i(j+1, k, l) = \theta^i(j, k, l) + C(i)\phi(i)$
        and use the above $\theta^i(j+1, k, l)$ to compute
        new $J(i, j+1, k, l)$ i.e., step 4D)
        iii. Else $m = N_S$

(F) Go to next bacterium $(i + 1)$ till all the bacteria undergoes chemotaxis i.e., go to step 4A)

Step 5: Reproduction
    a. For the given k and l, for each $i = 1, 2, 3, \ldots\ldots, S$, let $J_{health}^i = \sum_{j=1}^{j=N_c+1} J_{sw}(i, j, k, l)$ be the health of ith bacterium and sort J_{health} in ascending order.
    b. The bacteria with the highest J_{health} values die and those with minimum values split and the copies that are made already, now placed at the same location as their parent.

Step 6: If $k < N_{re}$, go to step 2. In this case, we have not reached the number of specified reproduction steps, so we start the next generation in the chemotactic loop.

Step 7: Elimination–dispersal: For $i = 1, 2, 3, \ldots\ldots, S$, a random number is generated and if it is less than or equal to P_{ed}, then that bacterium is dispersed to a new random location else it remains at its original location.

Step 8: If $l < N_{ed}$, then go to step 1; otherwise end.

The following BFA parameters are used in this work:

Chemotaxis loop counter = 200
Reproduction loop counter = 4
Elimination and dispersal loop counter = 2
Population size = 50
Elimination and dispersal probability = 0.25

The BFA flowchart is represented in Fig. 5.

5. Results and discussion

A MATLAB/SIMULINK model is developed to test the algorithms presented above. The parameters such as open circuit voltage (V_{oc}), short circuit current (I_{sc}), maximum power point voltage (V_{mp}), maximum power point current (I_{mp}), voltage temperature coefficient (k_v), and current temperature coefficient (k_i) are available in the manufacturer's datasheet. However, these values are insufficient to model solar PV characteristics accurately and it requires values of model parameters such as a, R_s, and R_p. These values are obtained using GA, AIS, and BFA methods.

The initial guesses of the model parameters are chosen randomly within the specified limit. The values of series resistance (R_s) are usually observed to be very small which makes it more appropriate to be defined within a limit of [0:2]. The boundaries of parallel resistance (R_p) are chosen as [50:500] due to its high value in nature. The diode ideality factor (a) is preferred between the limits [1:2].

With the above inputs, the MATLAB/SIMULINK model is simulated for three algorithms. After several runs, the best convergence characteristics of each method are obtained. Based on the convergence characteristics, the accuracy of the method is estimated in terms of minimal fitness values obtained after all the iterations. One such convergence characteristics obtained for BFA is presented in Fig. 6. From the fitness curve, it is clear that the best fitness value obtained with BFA is 0.0000049 which is very low compared to other two methods. Further, it also indicates that the convergence starts with lowest value of 1.6×10^{-3} and converges at a steady pace; finally reaching global optimum irrespective of initial guess. Hence, this proposed algorithm can be used in places where there is no prior knowledge about system variables.

5.1. Validation of model parameters obtained using BFA

It is impractical to change the values of model parameters every time for change in environmental conditions. So the model parameter values obtained should be almost constant for different environmental conditions unlike given in Ishaque and Salam (2011). Moreover, the value of series resistance is usually observed to be very small and parallel resistance should be high. Some of the data given in Ishaque and Salam (2011) is in contradiction to this basic idea. Table 1 shows the values of model parameters obtained for BFA under different temperature for three different types of panels namely Mono-crystalline (SM55), Thin film (Shell ST40) and Multi-crystalline (Shell S36). From the table one can be observe a small variation in value of series resistance (R_s) for three different makes. Further, from the comparison it is evident that the value of R_s is around 1 for thin film and less than 0.4 for both Multi-crystalline and Mono-crystalline. This result agrees well with the results presented in Ismail et al. (2013), where effect on solar PV characteristics with variation in R_s has been discussed. According to which, lower values of R_s makes the $I–V$ characteristic's to move away from the axis with respect to maximum point and vice versa with higher values. This tendency occurs naturally with the BFA parameter values.

5.2. Validation of the BFA results with experimental data

The model parameters extracted are subsequently substituted in the MATLAB/SIMULINK model to plot the $I–V$ characteristics of solar PV modules. Three different
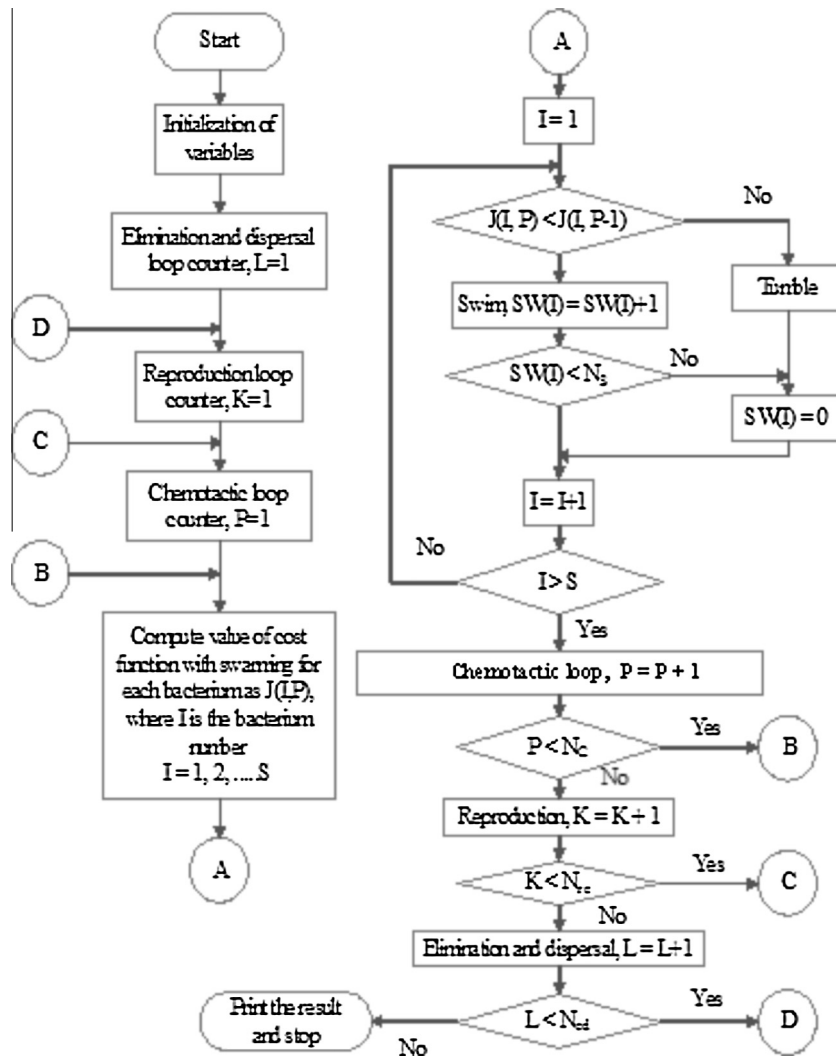
Fig. 5. Flowchart of BFA.

Table 1
Parameter values obtained with BFA for different temperature.

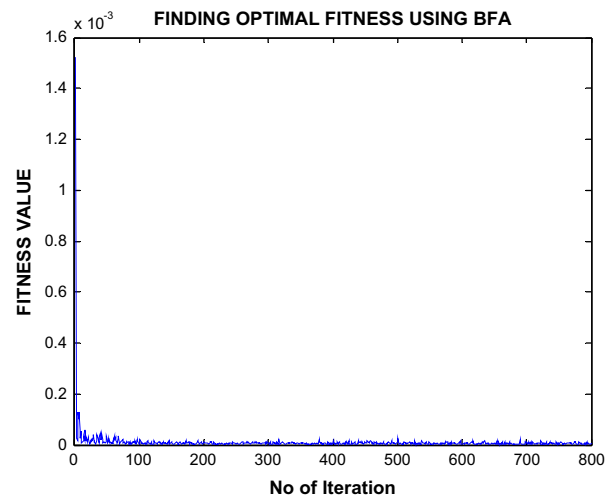| Parameters	S36	ST40	SM55
$T = 25\,°C$			
R_s	0.1281	1.01	0.339
R_p	479.4748	370.9784	454.1947
a'	1.6959	1.6489	1.3582
$T = 40\,°C$			
R_s	0.143	1.1821	0.3068
R_p	352.5868	346.4092	360.0138
a	1.6846	1.7129	1.4038
$T = 60\,°C$			
R_s	0.1102	1.03	0.3398
R_p	443.0576	349.5159	396.7666
a	1.5558	1.91	1.355

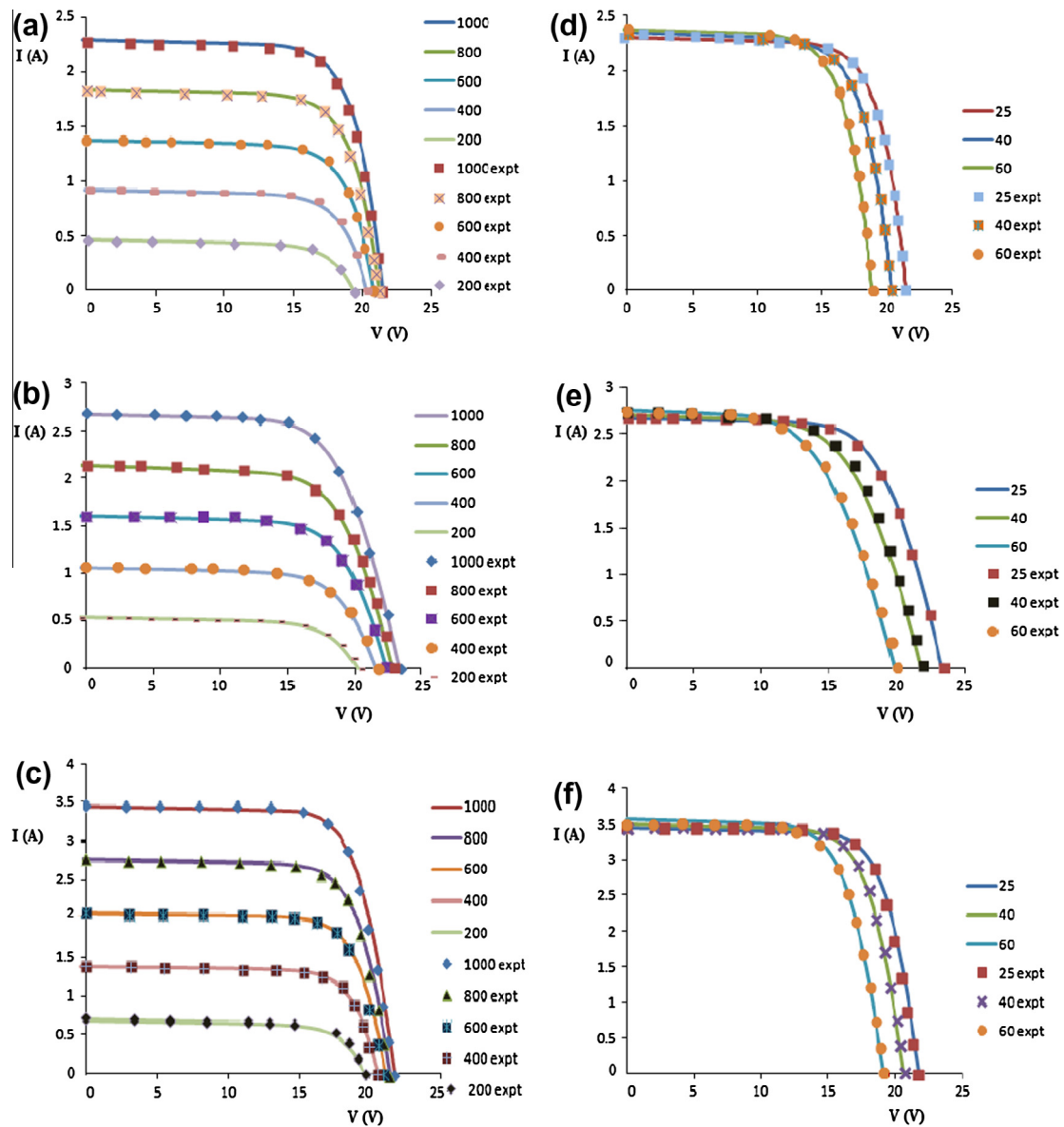Fig. 6. Variation of objective function with BFA method.

Fig. 7. The comparison of the experimental data with *I–V* curves obtained with BFA. (a) Shell S36 at different irradiation. (b) Shell ST40 panel at different irradiation. (c) Shell SM55 at different irradiation. (d) Shell S36 at different temperature. (e) Shell ST40 at different temperature. (f) Shell SM55 at different temperature.

panels are considered in this work for the evaluation of data obtained from BFA: Mono-crystalline (SM55), Thin film (Shell ST40) and Multi-crystalline (Shell S36). For comparison, experimental data are also extracted from manufacturer's datasheet for the same PV modules.

Since, BFA is superior to other methods, the computed solar characteristics of BFA alone is compared with the experimental data for different irradiation. The comparison of the experimental data with the *I–V* characteristics obtained with BFA algorithm for different irradiation and temperature are shown in Fig. 7a–e. From Fig. 7a–e, it is evident that the characteristics of solar PV obtained using BFA are exactly matching with the experimental values obtained from the datasheet. In comparison with (Ishaque and
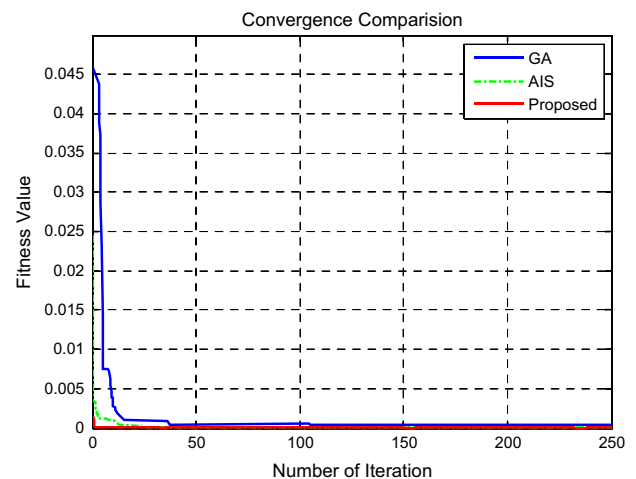

Fig. 8. Combined convergence characteristics of GA, AIS, and BFA.

Table 3
Comparison of GA, AIS and BFA.

Evaluation criteria	GA	AIS	BFA
Accuracy of solution	Low	Medium	High
Speed of convergence	High	High	Low
Consistency of solution	Medium	Medium	High
Computational efficiency	Low	Medium	High

Salam, 2011), the results obtained with the proposed method are more accurate and exhibit exact characteristics.

6. Comparison with GA and AIS methods

It is interesting to compare the proposed BFA algorithm with GA and AIS methods. This comparison is mandatory since GA is first proposed to predict I–V characteristics of solar panel. Further comparison with AIS helps to compute the efficacy of the proposed method. For fair comparison, all methods are terminated at 250th iteration and starts with random initial guess.

The combined convergence characteristics of all the methods are plotted and shown is in Fig. 8. Since all the methods are population based methods; they start with a set of solutions and converge to an optimal value. Among all the methods BFA starts with lowest value of objective function and converges at a steady pace. Further BFA converges at 120th iteration whereas GA and AIS converges at 80th and 110th iteration respectively. However, among the methods, BFA takes little more time to yield the best results. The accuracy obtained from the BFA outweighs the drawback of low speed of convergence. The initial guesses of these optimization algorithms are random in

nature which yields to poor performance in some runs. However, BFA gives good quality results in each run which makes the consistency of solution better.

Furthermore, comparison on model parameter obtained with different methods is presented in Table 2 for three different panels at different irradiation. From the table, it can be seen that the variation of computed model parameters using BFA are closer at different irradiation. For instance, the value of R_s is closer to value 1 for shell ST 40 panel, the value of R_p is nearer to 470 for shell S36 panel, the value of a is approximately equal to value 1.389 for shell SM55 panel. All this indicates that, the values of model parameters are observed to be nearly constant for all environmental conditions matching exactly with the theoretical prediction of smaller series resistance and higher parallel resistance.

6.1. Estimation of absolute error

To predict the closeness of the results obtained, absolute error is estimated for the proposed and GA method. Absolute error is computed using the following equation.

$$\text{Absolute error} = [I_{\text{experimental}} - I_{\text{computed}}] \qquad (19)$$

The computed absolute error graph for three different panels is presented in Fig. 9a–f. To maintain higher level of accuracy and clarity, the results are compared at same points. Two regions are identified for the comparison purposes.

1. The region to the left of MPP in solar I–V characteristics. i.e., Constant current region

Table 2
Variation of model parameter values obtained using GA, AIS, BFA under different irradiation.

| Parameters	Multicrystalline S36			Thin film ST40			Monocrystalline SM55		
	GA	AIS	Proposed Model using BFA	GA	AIS	Proposed Model using BFA	GA	AIS	Proposed Model using BFA
G = 1000 w/m²									
a	1	1.1769	1.6959	1	1	1.6489	1	1.7322	1.3782
R_s	0.4148	0.4555	0.1281	1.6540	1.36854	1.01	0.4614	0.3558	0.339
R_p	200.391	349.9511	478.4748	457.4780	461.3881	370.9784	416.4223	200	454.1947
G = 800 w/m²									
a	1	1	1.7931	1.8338	1.3881	1.6234	1.1261	1.4702	1.3824
R_s	0.6041	0.6706	0.0414	1	1.2473	1.01	0.2	0.5024	0.3191
R_p	461.3881	313.7890	489.8589	372.4340	100	370.9784	224.8289	200	318.8889
G = 600 w/m²									
a	1	1.2121	1.7491	1.7243	1.9511	1.6496	1.4897	1.5992	1.397
R_s	0.6178	0.4575	0.0216	1.2199	1	1.0027	0.262	0.5083	0.3127
R_p	207.2336	396.8719	475.3372	162.2678	278.5924	299.2976	200	267.8397	421.6824
G = 400 w/m²									
a	1	1.2708	1.6756	1.3607	1.9668	1.6547	1.6344	1.5093	1.3752
R_s	0.8074	0.2014	0.0867	1.8495	1.1926	1	0.6061	0.6393	0.3278
R_p	441.8377	234.6041	479.3708	372.4340	337.2434	309.5164	453.5679	257.089	457.0585
G = 200 w/m²									
a	1	1	1.6043	1.5797	1.74	1.6297	1	1.4936	1.4079
R_s	0.3891	0.5220	0.02	1.1144	1.6696	1.0187	0.2111	0.567	0.3
R_p	451.6129	375.3666	486.3113	193.5484	200	384.6959	200	260.0196	271.8618
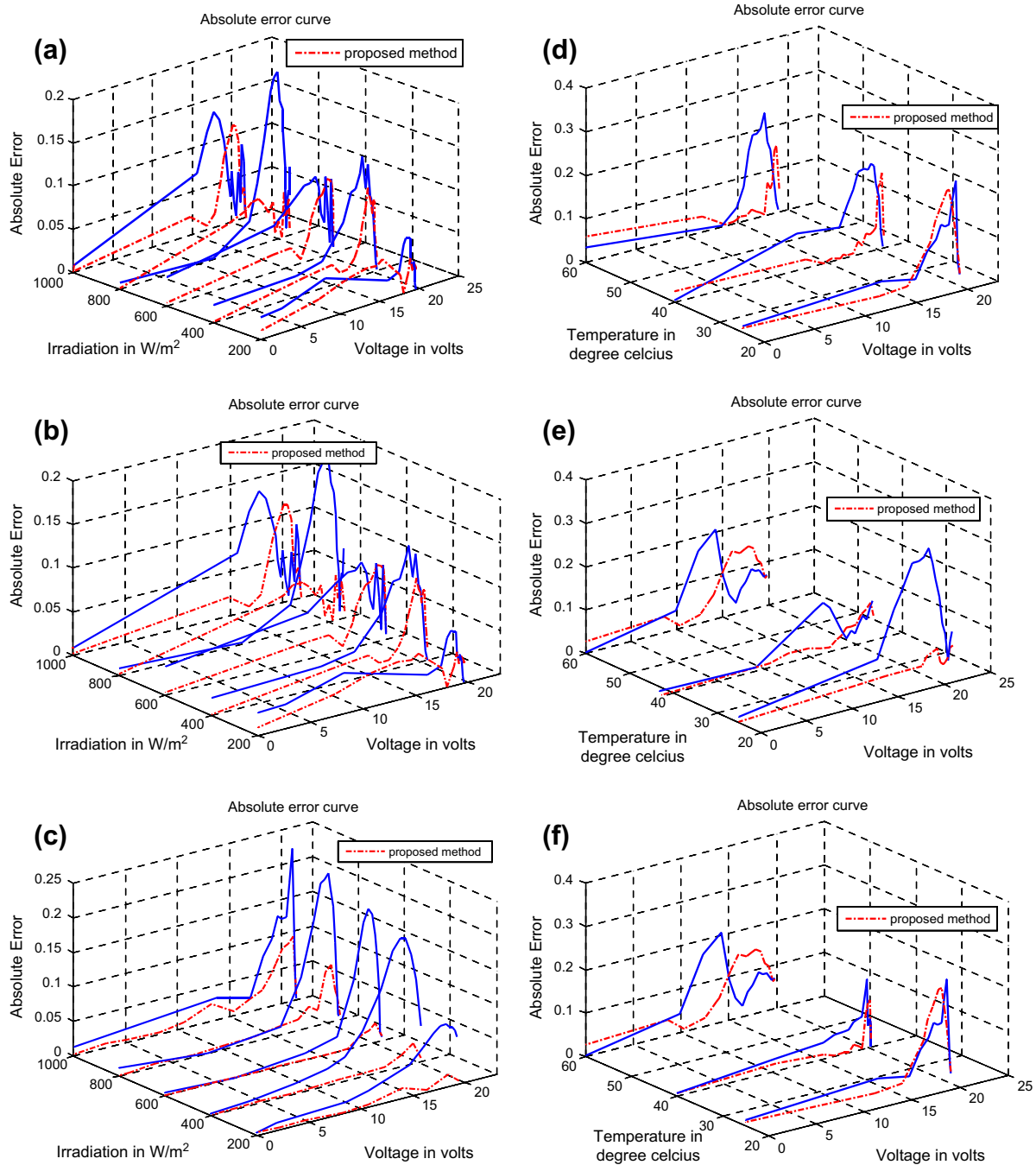
Fig. 9. Comparison of absolute error obtained using proposed method with GA. (a) SM55 at different irradiation. (b) ST40 at different irradiation. (c) S36 at different irradiation. (d) SM55 at different temperature. (e) ST40 at different temperature. (f) S36 at different temperature.

2. The region to the right of MPP i.e., Constant voltage region.

Generally, the error obtained in region 1 is less; because of the constant value of current. However, the error in region 2 is usually decides the accuracy and efficacy of any method. Fig. 9a–c shows the comparison of absolute error for different irradiation at constant temperature. Fig. 9d–f shows absolute error for different temperature at constant irradiation.

In both the cases, one interesting observation is error is minimal for both the methods at constant current region i.e. region 1. However, the difference arises in constant voltage region i.e. region 2. BFA provides lesser absolute error in comparison with GA in constant voltage region. This could be expected since BFA tries to find global optimum whereas GA only locates near global optimum. Both the methods exhibit similar characteristics at higher irradiation.

Based on Accuracy of solution, speed of convergence, consistency of solution, computational efficiency a compar-

ison table is made for all the three methods and is presented Table 3. From the table, it is clear that BFA provides accurate results with higher consistency, better computational efficiency compared to other two methods.

7. Conclusion

In this paper, BFA is proposed to determine three model parameters R_s, R_p and a accurately. Three different solar panel characteristics are obtained using BFA and the performance of BFA is compared with GA and AIS. Further, Solar photovoltaic I–V characteristics obtained from the simulation model is validated with experimental data extracted. The absolute error curve is plotted for BFA in comparison with GA and the error obtained in BFA is observed to be lesser. Based on consistency of solution, accuracy, computational efficiency, speed of convergence etc. it is found that BFA is the best computational method for extraction of model parameters.

References

Askarzadeh, Alireza., Rezazadeh, Alireza., 2012. Parameter identification for solar cell models using harmony search-based algorithms. Sol. Energy 86, 3241–3249.

Chan, D.S.H., Phang, J.C.H., 1987. Analytical methods for the extraction of solar-cell single- and double-diode model parameters from I–V characteristics. IEEE Trans. Electron. Dev. 34, 286–293.

da Costa, W.T., Fardin, J.F., et al., 2010. Identification of photovoltaic model parameters by differential evolution, IEEE International Conference on Industrial Technology (ICIT).

De Soto, W., Klein, S.A., Beckman, W.A., 2006. Improvement and validation of a model for photovoltaic array performance. Sol. Energy 80, 78–88.

Eslamian, Morteza, Hosseinian, Seyed Hossein, Vahidi, Behrooz, 2009. Bacterial foraging-based solution to the unit-commitment problem. IEEE Trans. Power Syst. 24 (3).

Farmer, D., Packard, N.H., Perelson, A.A., 1986. The Immune system adaptation and machine learning, Physica, 22D, pp. 187–204.

Goldberg, D.E., 2000. Genetic Algorithms in Search, Optimization, and Machine.

Holland, J., 1975. Adaptation in Natural and Artificial Systems. MIT Press.

Ishaque, K., Salam, Z., 2011. An improved modelling method to determine the model parameters of photovoltaic (PV) modules using differential evolution. Sol. Energy 85, 2349–2359.

Ishaque, K., Salam, Z., Syafaruddin, 2011a. A comprehensive MATLAB Simulink PV system simulator with partial shading capability based on two-diode model. Sol. Energy 85, 2217–2227.

Ishaque, K., Salam, Z., et al., 2011b. Simple, fast and accurate two-diode model for photovoltaic modules. Sol. Energy Mater. Sol. Cells 95 (2), 586–594.

Ismail, M.S., Moghavvemi, M., Mahlia, T.M.I., 2013. Characterization of PV panel and global optimization of its model parameters using genetic algorithm. Energy Convers. Manage. 73, 10–25.

Jervase, J.A. et al., 2001. Solar cell parameter extraction using genetic algorithms. Meas. Sci. Technol. 12 (11).

Jian, A., Kapoor, A., 2004. Exact analytical solutions of the parameters of real solar cells using Lambert W-function. Sol. Energy Mater. Sol. Cells 81 (2), 269–277.

Macabebe, E.Q.B., Sheppard, C.J., van Dyk, E.E., 2011. Parameter extraction from I–V characteristics of PV devices. Sol. Energy 85, 12–18.

Michalewicz, Z., 1994. Genetic Algorithms + Data Structures = Evolution Program, 2nd ed. Springer-Verlag, Berlin.

Mishra, S., 2005. A hybrid least square-fuzzy bacterial foraging strategy for harmonic estimation. IEEE Trans. Evol. Comput. 9 (1).

Mishra, S., Bhende, C.N., 2007. Bacterial foraging technique-based optimized active power filter for load compensation. IEEE Trans. Power Delivery 22 (1), 457–465.

Moldovan, N., Picos, R., et al., 2009. Parameter extraction of a solar cell compact model using genetic algorithms, CDE 2009. Electron. Dev., Spanish Conference.

Ortiz-Conde, A., García Sánchez, F.J., Muci, J., 2006. New method to extract the model parameters of solar cells from the explicit analytic solutions of their illuminated I–V characteristics. Solar Energy Mater. Solar Cells 90, 352–361.

Passino, K.M., 2002. Biomimicry of bacterial foraging for distributed optimization and control. IEEE Control Syst. Mag., 52–67.

Romero, B., del Pozo, G., Arredondo, B., 2012. Exact analytical solution of a two diode circuit model for organic solar cells showing S-shape using Lambert W-functions. Sol. Energy 86 (10), 3026–3029.

Villalva, M.G., Gazoli, J.R., et al., 2009. Comprehensive approach to modelling and simulation of photovoltaic arrays. IEEE Trans. Power Electron. 24 (5), 1198–1208.

Walker, G., 2001. Evaluating MPPT converter topologies using a MATLAB PV model. Aust. J. Elect. Electron. Eng. 21, 8.

Xiaoping, Chen, Bo, Qu, Gang, Lu, 2003. An application of immune algorithm in FIR filter design, IEEE International Conference.

Yang Fu-gang, 2010. An Improved Artificial Immune Algorithm, Sixth International Conference on Natural Computation (ICNC 2010).

Ye, M., Wang, X., et al., 2009. Parameter extraction of solar cells using particle swarm optimization. J. Appl. Phys. 105 (9), 094502–094508.

Zagrouba, M., Sellami, A., Bouaïcha, M., Ksouri, M., 2010. Identification of PV solar cells and modules parameters using the genetic algorithms: application to maximum power extraction. Sol. Energy 84, 860–866.